



HAL
open science

Interplay between Orientation at Electrodes and Copper Activation of *Thermus thermophilus* Laccase for O₂ Reduction

Vivek Pratap Hitaishi, Romain Clément, Ludovica Quattrocchi, Philippe Parent, David Duché, Lisa Zuily, Marianne Ilbert, Elisabeth Lojou, Ievgen Mazurenko

► To cite this version:

Vivek Pratap Hitaishi, Romain Clément, Ludovica Quattrocchi, Philippe Parent, David Duché, et al.. Interplay between Orientation at Electrodes and Copper Activation of *Thermus thermophilus* Laccase for O₂ Reduction. *Journal of the American Chemical Society*, 2020, 142 (3), pp.1394-1405. 10.1021/jacs.9b11147 . hal-02503732

HAL Id: hal-02503732

<https://hal.science/hal-02503732v1>

Submitted on 10 Mar 2020

HAL is a multi-disciplinary open access archive for the deposit and dissemination of scientific research documents, whether they are published or not. The documents may come from teaching and research institutions in France or abroad, or from public or private research centers.

L'archive ouverte pluridisciplinaire **HAL**, est destinée au dépôt et à la diffusion de documents scientifiques de niveau recherche, publiés ou non, émanant des établissements d'enseignement et de recherche français ou étrangers, des laboratoires publics ou privés.

Interplay between orientation at electrodes and copper activation of *Thermus thermophilus* laccase for O₂ reduction

Vivek Pratap Hitaishi,^{†,‡} Romain Clément,^{†,‡} Ludovica Quattrocchi,^{†,‡} Philippe Parent,[§] David Duché,^{||} Lisa Zuily,^{†,‡} Marianne Ilbert,^{†,‡} Elisabeth Lojou,^{†,‡,*} Ievgen Mazurenko^{†,‡,*}

[†] Aix Marseille Univ, CNRS, BIP UMR 7281, 31 Chemin Aiguier, CS 70071, 13402 Marseille Cedex 09, France

[‡] Aix Marseille Univ, CNRS, IMM FR 3479, 31 Chemin Aiguier, CS 70071, 13402 Marseille Cedex 09, France

[§] Aix Marseille Univ, CNRS, CINAM UMR 7325, Campus de Luminy, 13288 Marseille Cedex 09, France

^{||} Aix Marseille Univ, Université de Toulon, CNRS, IM2NP UMR 7334, 13397 Marseille, France

Corresponding authors e-mails : lojou@imm.cnrs.fr; imazurenko@imm.cnrs.fr

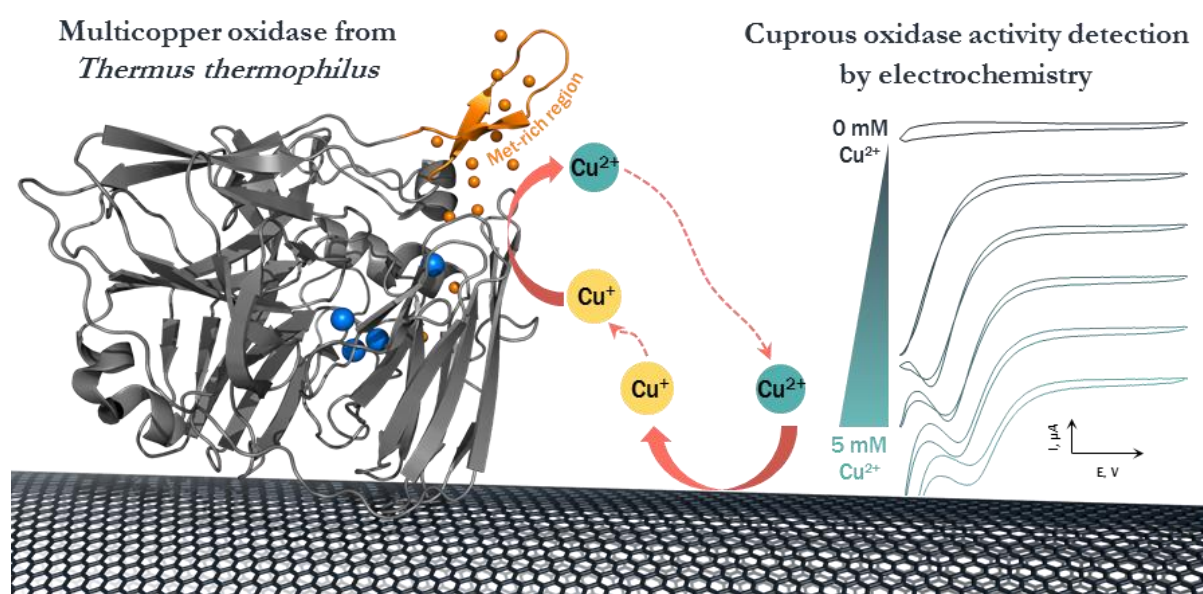
KEYWORDS: *Enzyme; catalysis; electrochemistry; copper; cuprous oxidase; multicopper oxidase; laccase; carbon nanotube; self-assembled monolayer;*

This document is the unedited Author's version of a Submitted Work that was subsequently accepted for publication in Journal of the American Chemical Society, copyright © American Chemical Society after peer review. To access the final edited and published work see <https://pubs.acs.org/doi/10.1021/jacs.9b11147>

ABSTRACT:

Multicopper oxidases (MCOs) catalyze the oxidation of a variety of substrates while reducing oxygen into water through four copper atoms. As an additional feature, some MCOs display an enhanced activity in solution in the presence of Cu²⁺. This is the case of the hyperthermophilic laccase HB27 from *Thermus thermophilus*, the physiologic role of which is unknown. As a particular feature, this enzyme presents a methionine rich domain proposed to be involved in copper interaction. In this work, laccase from *T. thermophilus* was produced in *E. coli*, and the effect of Cu²⁺ on its electroactivity at carbon nanotube modified electrodes was investigated. Direct O₂ electroreduction is strongly dictated by carbon nanotube surface chemistry in accordance with the enzyme dipole moment. In the presence of Cu²⁺, an additional low potential cathodic wave occurs, which was never described earlier. Analysis of this wave as a function

of Cu^{2+} availability allows us to attribute this wave to a cuprous oxidase activity displayed by the laccase and induced by copper binding close to the Cu T1 center. A mutant lacking the methionine-rich hairpin domain characteristic of this laccase conserves its copper activity suggesting a different site of copper binding. This study provides new insight into the copper effect in methionine rich MCOs, and highlights the utility of the electrochemical method to investigate cuprous oxidase activity and to understand the physiological role of these MCOs.



INTRODUCTION

Enzymes from multicopper oxidase (MCO) family oxidize a wide variety of substrates with the concomitant reduction of oxygen into water. Some are particularly well described, namely laccases, bilirubin oxidases (BODs) and copper efflux oxidases (CueO). They all contain four copper atoms, spatially organized in two sites. The electrons are transferred from the Cu type 1 (T1) substrate-binding site to a trinuclear center, composed of one T2 Cu and two T3 Cu, where O_2 is reduced into water.^{1,2} Most laccases have a low substrate specificity allowing them to catalyze the oxidation of various aromatic substrates and thus being potentially involved in industrial bioremediation processes.

Thermus thermophilus HB27 Laccase (*Tt* Lac) is a 53 kDa protein³ identified in this extremely thermophilic bacterium and first crystallized in 2011.⁴ A particular hairpin located near Cu T1 and accommodating 6 out of 13 methionines available in the enzyme sequence was identified.⁵ Methionine rich region is a particular feature of the proteins involved in copper homeostasis, notably CueO from *E. coli* which is a MCO sharing 30.8% identity with *Tt* Lac.³ CueO confers cells resistance in copper stress environment, to protect cells it is believed to act as an efficient copper oxidase able to detoxify the periplasm from toxic cuprous ions.⁶⁻⁸ The Met-rich region of CueO is supposed to hamper the binding of bulky organic substrates, such as 2,2'-azino-bis-(3-ethylbenzthiazoline-6-sulfonate (ABTS)), a model substrate of laccases.⁹ In agreement, deletion of the Met-rich domain induced a 10-fold increase in the activity in solution towards ABTS.^{9,10} As a notable property of *Tt* Lac, shared with CueO, its activity in solution was shown to be enhanced by the presence of exogenous cupric ions. Actually, a fifth Cu atom (sCu for substrate Cu) was revealed in the structure of CueO in the presence of Cu²⁺, located at one extremity of the Met-rich helix close to Cu T1.^{11,12} This copper is labile, and the occupancy of the sCu-site strongly depends on the environment conditions, e.g. on the affinity of the buffer for Cu²⁺.¹³ The dissociation constant for Cu⁺ at the sCu-site was 4 orders of magnitude smaller than that of Cu²⁺, and CueO would function as laccase, i.e. phenol oxidase, only when a copper atom occupies the sCu-site. Later, at least two other potential Cu-binding sites, located in the Met-rich helix and much more exposed to the solvent than the sCu-site, were identified.^{12,14} These Cu-binding sites are situated less than 13 Å from the sCu-site or from each other, a distance that is compatible with electron transfer (ET).¹⁵ They were proposed to play a role in copper detoxification, performing Cu⁺ fixation and oxidation by ET to the Cu T1 buried in the protein.

E. coli CueO has been studied on various electrochemical interfaces, although far less reports can be found compared to other laccases and BODs.¹⁶⁻²⁵ Kano *et al.* reported early in 2007 the

electrochemistry of CueO adsorbed on a pyrolytic graphite electrode.¹⁶ The catalysis of O₂ reduction was observed in the absence of redox mediators, a process called direct electron transfer (DET) process in contrast with mediated one. Direct catalysis of O₂ reduction occurred with an onset of 0.35 V vs Ag/AgCl at pH 5, suggesting that this enzyme should be classified as middle redox potential MCO due to the methionine coordination of Cu T1 center.¹ No effect of Cu²⁺ on the catalysis was detected, and an ET pathway directly from the electrode to the Cu T1 was proposed.¹⁶ Non catalytic redox signals attributed to Cu T1 were only observed for the Met-rich helix deletant of CueO, suggesting that Cu T1 was more accessible after helix deletion.⁹ However, the non catalytic redox wave at +0.28 V vs Ag/AgCl attributed to Cu T1 was later observed for WT *E. coli* CueO adsorbed on more porous carbon aerogel.¹⁷ The electrochemical studies realized thereafter on CueO did not take into consideration or even mentioned the Met-rich helix.¹⁸⁻²¹

Even less studies reported the behavior of *Tt* Lac on electrochemical interfaces. The first study was realized in 2011 with *Tt* Lac drop casted from an agarose solution on glassy carbon electrodes.²⁶ Activity was tentatively measured at pH 4.5 in the presence of ABTS, but no clear catalytic current was observed. Harry Gray *et al.* reported the direct wiring of *Tt* Lac on Ketjen black modified by pyrenebutyric acid.²⁷ In the absence of redox mediators and additional copper, the catalysis of O₂ reduction occurred with an onset of 0.34 V vs Ag/AgCl at pH 5. This value matched the redox potential of Cu T1 whose non catalytic cathodic and anodic peaks were observed at 0.3 and 0.36 V vs Ag/AgCl respectively. Further, the same group reported the kinetic modeling of O₂ reduction by *Tt* Lac.²⁸ They showed that the average distance of Cu T1 to the electrode for *Tt* Lac immobilized on Ketjen black was 24-28 Å. No influence of copper addition was investigated.

This literature survey emphasizes the complexity of action of exogenous copper for these two MCOs, mostly investigated by biochemical studies in the aim to understand the interplay

between cuprous and phenol oxidase activities observed in different conditions. The similarities in the behavior and the structures of *Tt* Lac and *E. coli* CueO suggest a similar mechanism of copper-related phenomena, yet not completely deciphered for either of them from a biochemical point of view. The studies of these phenomena from an electrochemical point of view for both *E. coli* CueO and *Tt* Lac are lacking. The goal of this paper is to link biochemical studies of the copper effect to electrochemical ones in order to get new insight in the mechanism of *Tt* Lac activation by copper. To this end, we take benefit of *Tt* Lac different electrochemical behavior depending on the charge of nanostructures used for enzyme immobilization on the electrode. We first determine the key parameters that drive the electrochemical wiring of *Tt* Lac, and propose an electrostatic model for oriented enzyme immobilization at the electrode interface. Then, and for the first time as far as we are aware, we report the electrochemical detection and analysis of the cuprous oxidase activity of *Tt* Lac in the presence of increasing amounts of Cu^{2+} , and as a function of enzyme orientation. The influence of the Met-rich domain in *Tt* Lac is considered using the wild type (WT) enzyme and a hairpin deletant of *Tt* Lac. We propose two different ET pathways between *Tt* Lac and the electrode, one linked to the direct wiring of *Tt* Lac through the Cu T1, and another linked to the ET from the electrode to Cu T1 through the exogenous copper cation bound to protein.

EXPERIMENTAL SECTION

Chemicals and materials. Ethanol analytical grade 96% (v/v), 2,2'-azino-bis(3-ethylbenzothiazoline-6-sulfonic acid) (ABTS), 6-mercaptohexanoic acid (6-MHA), cysteamine (CYST), bathocuproine disulfonate anion (BCS), ethylenediaminetetraacetic acid (EDTA), 6-mercapto-1-hexanol (OH), N-methyl-2-pyrrolidone (NMP), sodium fluoride 99% (NaF), sodium acetate (NaAc), acetic acid (CH_3COOH), sodium hydroxide 97 % (NaOH), sulfuric acid 95-98 % (H_2SO_4), copper (CuSO_4), zinc (ZnSO_4), nickel (NiSO_4) and calcium (CaSO_4) sulfate solutions were purchased from Sigma-Aldrich. 1,4-Diethylpiperazine (DEPP) was from

Alfa Aesar. All chemicals for protein purification are high purity products from Sigma-Aldrich. Sodium acetate buffer solutions were prepared by mixing NaAc and acetic acid in an appropriate ratio to obtain desired pHs and a final buffer concentration of 100 mM. DEPP buffer was prepared by adding H₂SO₄ to DEPP solution (pK₁ = 4.48; pK₂ = 8.58) until the desired pH is reached. All solutions were prepared with Milli-Q water (18.2 MΩ cm). BOD from *Bacillus pumilus* (*Bp* BOD) was a gift from Dr Nicolas Mano (CRPP, Bordeaux, France).²⁹ Two types of carbon nanotubes (CNT) were used for enzyme immobilization. Carboxylic-functionalized multiwalled carbon nanotubes (hereafter denoted as Neg-CNTs) were purchased from NanoLab Inc. (U.S.A.) and dispersions (2 mg/mL) were prepared in Milli-Q water by sonicating for 1 hour. Amino-functionalized multiwalled carbon nanotubes (hereafter denoted as Pos-CNTs) were purchased from DropSens (Spain) and dispersions (2 mg/mL) were prepared in NMP:Milli-Q water (1:1) by sonicating for 4 hours.

Cloning, expression and purification of *Tt* Lac. The gene encoding for *Tt* Lac (strain *T. thermophilus* HB27) was amplified from *T. thermophilus* chromosome with primers PRC1 and PRC2 (Table S1). The plasmid pet21b (Addgene, Cambridge, USA) was linearized with primers PRC3 and PRC4 (Table S1). *Tt* Lac gene was inserted into pet21b by ligation using the SLIC method described previously.³⁰ The plasmid obtained will be called pet21b-Ttlac. Site directed mutagenesis (pet21b-TtlacC445A) was performed with the QuickChange® Site-Directed Mutagenesis Kit (Stratagene, San Diego, USA) with primers PRC5 and PRC6 described in Table S1. For the hairpin mutant (pet21b-Ttlac_{hairpin}), primers PRC7 and PRC8 were used to linearize the plasmid while depleting the hairpin region. BamHI restriction sites were added at the extremity of each primer. After BamHI digestion of the PCR product, ligation was performed. Plasmids were transformed in *E. coli* DH5α and for protein production into *E. coli* Origami™ 2(DE3) strains (Merck Millipore, Burlington, USA). Plasmids were sequenced by Genewiz (Beckman Coulter Genomics Inc., Chaska, USA). *E. coli* strains containing the

required plasmid were grown in Luria-Bertani (LB) media (Merck, Darmstadt, Germany) with 200 µg/mL ampicillin, 25 µg/mL kanamycin and 25 µg/mL tetracycline.

E. coli Origami™ 2(DE3) cells containing pet21b-Ttlac wild type or mutants were grown at 37°C in aerobic condition up to OD_{600nm} 0.6. 500 µM IPTG was then added to induce gene expression. Temperature was decreased to 22°C, 500 µM CuSO₄ was added and cells were further incubated for 24 hours in aerobic condition followed by 24 hours in anaerobic condition as described by Durao and Gounel.^{29,31} Cells were harvested by centrifugation at 7200 g and frozen at -80°C.

Cell pellet was resuspended at 4°C in sodium phosphate buffer 50 mM pH 7.4 containing 500 mM NaCl and 10 mM imidazole (Buffer 1). Protease inhibitor, lysozyme and DNase were added. Cells were sonicated in ice for 1 minute with 60 s intervals (5 cycles) (Sonic & Material Inc, Bioblock, Danbury, USA). *Tt* Lac wild type or mutants were purified from the soluble fraction after two successive centrifugations (10,500 x g for 30 minutes and 140,000 x g for 30 minutes). The supernatant was loaded onto a His-Trap HP 1 ml column (GE Healthcare, Chicago, USA). Proteins were eluted with a step gradient of imidazole (50 mM, 250 mM and 500 mM imidazole). *Tt* Lac was eluted at 250 mM imidazole. Purified proteins were dialyzed against sodium phosphate buffer 100 mM pH 7.4 (Buffer 2) (dialysis tubing: 12-15 kDa pore size, Medicell Membrane Ltd, London, UK) during 1 night, and concentrated (Vivaspin®, 30kDa, Sartorius, Göttingen, Germany). SDS PAGE gel was performed to check the protein purity.

To remove the His-tag of *Tt* Lac, 1.5 mg/ml of purified protein was incubated in 20/1 concentration (mg/mg) of protease TEV (purified as described in SI) during one night at 4°C in 25 mM sodium phosphate buffer pH 8, 200 mM NaCl and 5 mM β-mercaptoethanol. After

digestion, *Tt* Lac with deleted His-tag was loaded onto a Ni-NTA column and collected in the unbound fractions while TEV protease was eluted at 500 mM imidazole.

Solution-based enzymatic assays. Enzymatic assays were performed at 30°C with spectrophotometer microplate reader (Spark 10M, Tecan, Männedorf, Swiss) by measuring absorption at 420 nm. Tests were performed with ABTS. Three technical replicates were performed. Copper activation was measured with 20 mM ABTS in 50 mM acetate buffer pH 5, with different CuSO₄ concentrations. Kinetic activity parameter was quantified with or without CuSO₄ with 0.25 μM *Tt* Lac WT, in 50 mM NaAc buffer pH 5, with different ABTS concentrations. ABTS kinetic parameters of the enzyme were calculated by Sigma-Plot (Systat Software Inc., San Jose, USA) with Michaelis-Menten equation with one site saturation: $V_i = (V_{\max} \times [S]_0) / (K_M + [S]_0)$ where V_i = initial speed, V_{\max} = maximal initial speed, K_M = Michaelis constant and $[S]_0$ = ABTS concentration.

Electrode Preparation. Two working electrodes were used throughout the study. A polycrystalline gold electrode (geometric surface of 0.008 cm²) was purchased from Bio-Logic Science Instruments. It was treated by thiol solutions as described in ³². A pyrolytic graphite electrode (PG electrode, geometric surface of 0.071 cm²) either bare or modified with different CNTs was also used. PG electrode cleaning and further surface modification was adapted as in ³³. Briefly, the PG electrode was polished by a wet emery paper (1200), sonicated in 30% ethanol solution for cleaning and dried prior to any further modification. 2 μL of Pos-CNT or Neg-CNT dispersion was drop casted on the pre-cleaned PG electrode and dried at 60°C. Modified electrodes show good adhesion and mechanical stability of the CNTs deposit which was confirmed by the stable catalytic response along with the electrochemical experiment.

For enzyme adsorption, unless otherwise indicated, both polycrystalline gold or PG electrodes either modified or unmodified were incubated for 15 min at 4°C with freshly prepared 10 μM

enzyme solution in 100 mM NaAc buffer at pH 5. Then enzyme modified electrode was gently washed with the same buffer to remove the loosely adsorbed enzymes, and transferred to the electrochemical cell containing 100 mM NaAc buffer pH 5 for further electrocatalytic experiments.

Electrochemistry measurements. Electrochemical measurements (Cyclic voltammetry (CV), and chronoamperometry) were performed in a standard 3-electrode cell (comprising a polycrystalline gold or a PG as a working electrode, a Hg/Hg₂SO₄ reference electrode (sat. K₂SO₄) and a Pt-wire auxiliary electrode) using a potentiostat from Autolab PGSTAT30 controlled by Nova software (Eco Chemie). All potentials are quoted vs Ag/AgCl reference electrode (sat. KCl) by adding 430 mV to the measured potential, they can further be converted to the values versus normal hydrogen electrode (NHE) by adding 197 mV. Current densities are reported to the geometrical surface of the electrodes. The cell was thermostated at 30 °C and oxygen was continuously bubbled into the cell throughout the experiments, unless otherwise specified. The anaerobic experiments were performed in the glove box.

CNT characterization. XPS experiments were performed on the SUMO UHV experimental setup for photoemission and surface infrared. The data were recorded under ultra-high vacuum using a Resolve 120 hemispherical electron analyzer (PSP Vacuum) and an unmonochromatized X-ray source (Mg K_α at 1253.6 eV, PSP Vacuum) operated at 124 W at an incidence angle of 30° with respect to the analyzer axis. A drop of CNT dispersion was deposited on a gold coated glass substrate, dried for 30 minutes at 50°C, then introduced into the experiment under UHV. The spectra were deconvoluted using Origin software. Zeta-potential measurements were made with Zetasizer from Malvern Panalytical in 100 mM NaAc buffer at desired pH using a disposable cell.

Structure analysis. Pymol 2 (Schrödinger, New-York, USA) was used to draw protein structures, to measure distances and to perform structure alignment. The electrostatic charge

distribution was calculated using a Pymol plugin APBS Electrostatics. The structure was prepared and atom charges and radiuses were assigned with PDB2PQR³⁴ using AMBER force field and PROPKA³⁵ to calculate the titration states at a particular pH. Ionic strength of 0.15 M and pH 5 were used by default in these calculations. Dipole moments were determined from the pqr output files using the Protein Dipole Moments Server.³⁶ Consurf server (<http://consurf.tau.ac.il/2016/>) was used to determinate the amino acid conservation degree.³⁷ Phyre2³⁸ was used to model protein structure of mutants. Clustal Omega and ESPript 3 were used to perform sequence alignment.^{39,40}

RESULTS AND DISCUSSION

Key parameters driving DET with *Tt* Lac. In MCOs, the usual entry site of electrons for catalysis was proved to be the Cu T1, which is the site where the physiological substrate binds. To get the highest interfacial ET rate, following Marcus theory, many works previously showed that the Cu T1 environment has to be placed at the shortest distance to the electrode surface.¹ Careful consideration of the 3D structure of the enzyme is required to determine the key parameters for its orientation on the electrode interface yielding direct electron transfer (DET). Figure 1 shows the crystallographic structure of *Tt* Lac with the surface amino acid residues colored as a function of their charges. The Cu T1 center is buried in the protein shell lying at the closest distance of *ca.* 11 Å from the surface region that shows a net negative charge under the Met-rich hairpin (magenta). On the opposite face of the molecule a net positive patch is present, inducing a significant dipole moment (878 D at pH 5, 965 D at pH 7) pointing opposite from the Cu T1. As a result, it is expected that immobilizing the enzyme on negatively charged interfaces will repel the Cu T1 surrounding, thus disfavoring DET, in a similar way as reported for *E. coli* CueO.²⁴

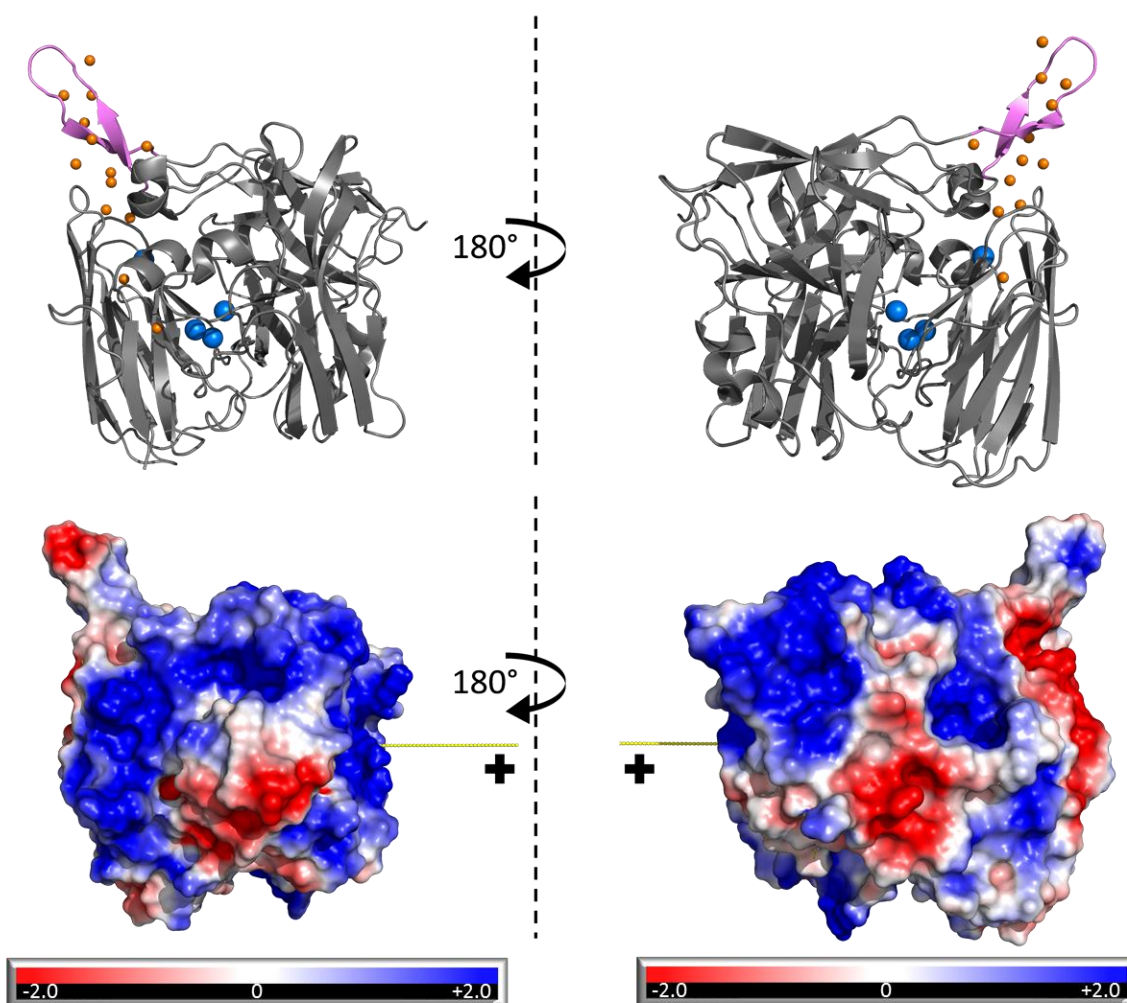


Figure 1: (top panel) 3D structure of *Tt* Lac (PDB 2XU9) showing the hairpin domain (magenta), T1 and T2/T3 Cu centers (blue spheres) and all Met sulfurs (yellow spheres). (bottom panel) Electrostatic charges at the surface of *Tt* Lac in the same orientation as on top panel at pH 5 with the following color code: positive charges in blue, negative charges in red, neutral in white. The positive end of the dipole moment vector is shown as a yellow stick and it is positioned in the image plane.

To firmly prove the orientation-driven DET process, the effect of electrode surface charges on DET was first evaluated by adsorption of *Tt* Lac on thiol-based self-assembled-monolayers (SAMs). Figure 2 gives the CVs obtained under O₂ atmosphere with *Tt* Lac adsorbed on carboxylic (COOH)-, hydroxyl (OH)-, or amino (NH₂)-terminated SAMs. At pH 5, according to their respective pK_a, these thiols generate a negative, neutral hydrophilic and positive surface, respectively. Considering the pI of *Tt* Lac (pI = 9.3) the enzyme surface is globally

positive at pH 5.⁴ Nevertheless, almost no catalytic signal on COOH-SAM, and only a weak catalytic current can be observed on OH-SAM. On the contrary, catalytic signals with current densities in the range of $60 \mu\text{A}\cdot\text{cm}^{-2}$ developed on NH_2 -SAMs. The onset potential for O_2 reduction on positive SAMs is +440 mV vs Ag/AgCl at pH 5. This value reflects the Cu T1 redox potential typical of a Met axial ligand.⁴¹

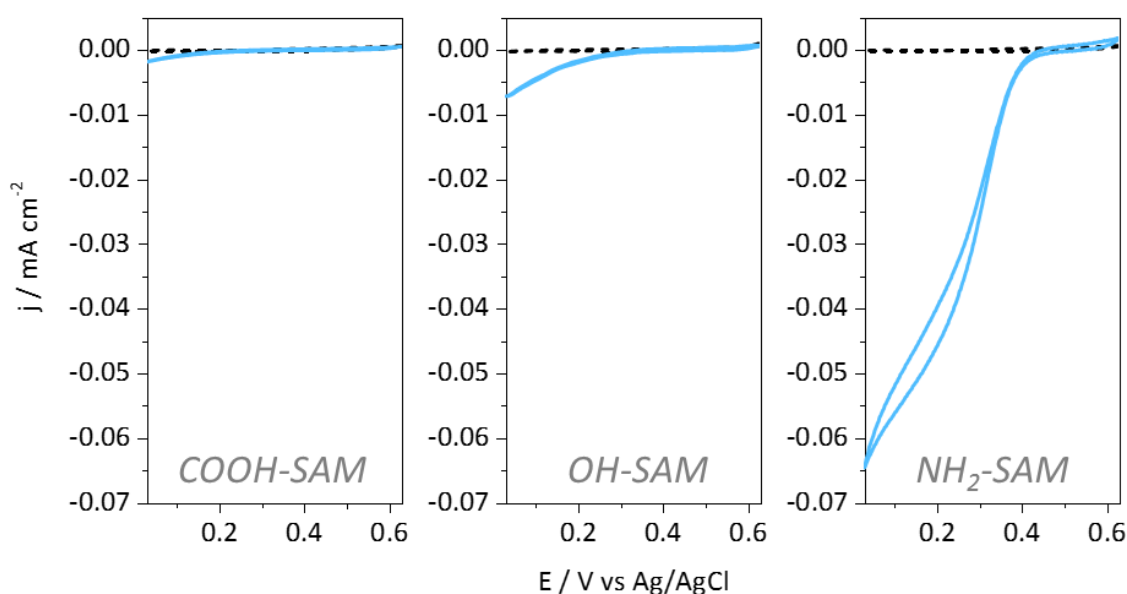


Figure 2: CV responses of O_2 reduction by Tt Lac adsorbed on different SAM-modified gold electrodes: 6-MHA (COOH-SAM), MH (OH-SAM), and CYST (NH_2 -SAM). Dashed lines represent SAM-modified gold electrodes without Tt Lac. 0.1 M NaAc buffer pH 5, scan rate 5 mV s^{-1} .

SPR and ellipsometry measurements highlight the presence of an enzyme layer with a thickness close to a monolayer whatever the SAM chemistry (Figure S1), meaning that the absence of catalytic current on COOH-SAM is not linked to an electrostatic repulsion preventing enzyme adsorption on the electrode surface. The favored DET process on the positive SAM and the absence of any DET on the negative one confirm the hypothesis based on the structure examination. Our results also emphasize the very similar electrochemical behavior of Tt Lac and *E. coli* CueO²⁴ as a function of the electrode surface charges.

***Tt* Lac adsorbed on carbon nanotubes with a positive zeta potential.** Carbon nanomaterials are often more suited for the enhancement of catalytic currents due to high surface area and the involvement of hydrophobic interactions with CNT-walls favoring the enzyme adsorption.⁴² *Tt* Lac was first adsorbed on a deposit of CNTs presenting a positive zeta potential, thus expected to favor enzyme orientation for DET. As reported in Table 1, this first CNT material (named thereafter Pos-CNT) contains less than 0.33% of carboxylic functionalities and comparable amount of amino functionalities, (Figure S2) yielding a positive zeta potential of +26 mV at pH 5.

	XPS Analysis									Zeta Potential (mV)		
	Elemental %			O _{1s} %				N _{1s} %		pH		
	C	N	O	C-O	C=O	O-C=O	H ₂ O	amine	N « graphitic »	3.6	5	7.5
Pos-CNT	98.57	0.31	1.12	0.53	0.25	0.33	0.00	0.31	0.00		26 ± 2.80	-7.29 ± 1.98
Neg-CNT	88.08	1.17	10.75	2.72	2.73	4.6	0.70	0.60	0.57	-26.8 ± 1.35	-30.7 ± 1.31	-25.6 ± 1.69

Table 1: Quantitative comparison of XPS data and values of zeta potential at different pHs for Pos-CNT and Neg-CNT.

Accordingly, with *Tt* Lac immobilized by adsorption on Pos-CNT, a DET catalytic process under O₂ occurs at an onset potential very close to the one observed on NH₂-SAM (Figure 3). No catalytic current can be observed in the absence of Lac, or under N₂. Despite pronounced DET process, we were unable to clearly isolate the non-catalytic signals of *Tt* Lac in anaerobic conditions (Figure S3), probably because of low coverage and large distance between T1 Cu and electrode.²⁸

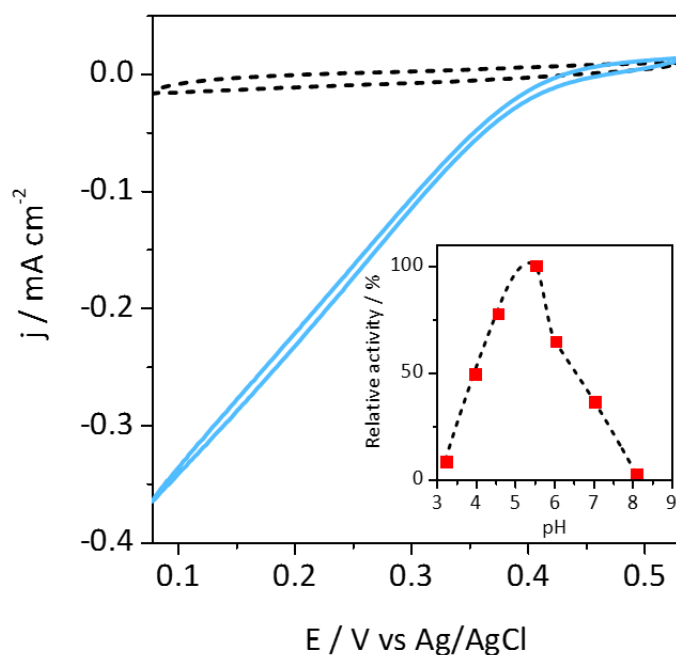


Figure 3: CVs at Pos-CNT in the presence of *Tt* Lac under O₂ (blue line) or N₂ (black dashed line). Electrode rotation speed 800 rpm, scan rate 5 mV s⁻¹. Inset: Relationship between *Tt* Lac relative activity and pH for O₂ catalytic reduction at the Pos-CNT.

Varying the rotation rate highlights no limitation of the catalytic current by mass transfer at observed current densities (Figure S4A). The relationship between the limiting catalytic current and pH displays a bell shape, with an optimum at pH close to 5, in agreement with the optimal pH determined by classical spectrophotometric assays (Figure 3, inset).³

The protein was produced with a His-tag at C-terminal end of the polypeptide. As a control, the protein with His-tag cleaved by TEV-protease was also studied on the Pos-CNT deposit. It displays a very similar behavior with the His-tagged enzyme, suggesting that this region is not involved in the electrode recognition (Figure S4B).

***Tt* Lac adsorbed on carbon nanotubes with a negative zeta potential.** The second type of CNTs we studied contains a high proportion of O atoms compared to Pos-CNT (10.75% vs

1.12%), mainly in the form of carboxylic functions (4.6%). The direct consequence is the large negative value of zeta potential at pH 5 (-30.7 ± 1.35 mV) (Table 1). These CNTs will be named Neg-CNTs. In agreement with our finding on SAMs, virtually no DET can be observed when *Tt* Lac was immobilized by adsorption on Neg-CNT (Figure 4).

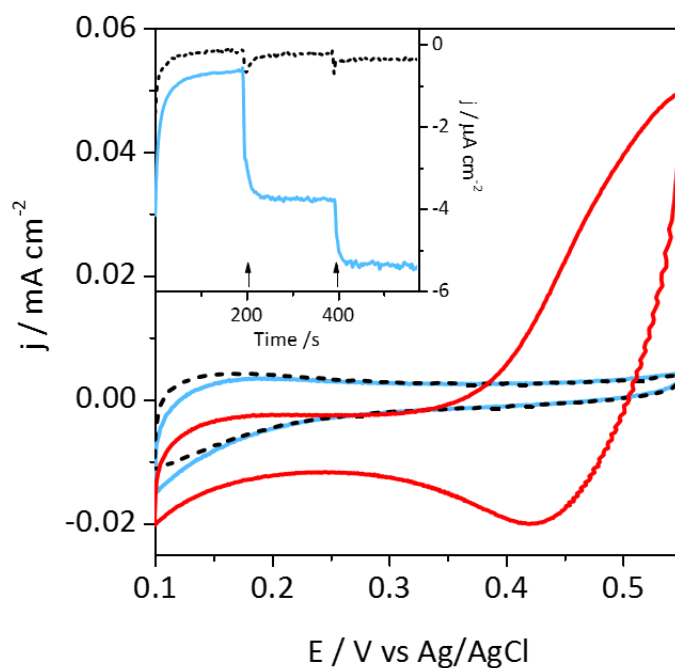


Figure 4: CVs for O_2 reduction on Neg-CNT in the absence of *Tt* Lac (black dashed line), in the presence of *Tt* Lac (blue solid line) and in the presence of *Tt* Lac and 1 mM ABTS (red solid line). 0.1 M NaAc buffer pH 5, scan rate 5 mV s^{-1} . Inset: chronoamperometry of O_2 reduction at 0.2 V in the absence (black dashed line) and in the presence of *Tt* Lac (blue solid line); 1 mM ABTS was added at 200 s and 400 s as indicated by arrows.

Adding redox mediators in solution is another way to connect artificially the enzymes, and to give access to the proportion of enzymes in an unfavored orientation for DET. However, using *Tt* Lac for O_2 reduction, only extremely weak MET currents below $5 \mu\text{A cm}^{-2}$ were recorded in the presence of ABTS, the classical redox mediator used in MCO spectrophotometric activity tests in solution (Figure 4). However, we measured a K_M 2.9 mM of *Tt* Lac for ABTS in

solution-based enzymatic assay at 30 °C (Table S2), i.e. 100 times higher than the K_M of another MCO *B. pumilus* BOD⁴³ that displays pronounced MET current in the same conditions (Figure S5). The high K_M value and low k_{cat} of *Tt lac* for ABTS ($k_{cat}/K_M \sim 10^2 \text{ M}^{-1} \text{ s}^{-1}$) suggest its low efficiency for this substrate oxidation and explains the weak MET. In analogy with *E. coli* CueO, it also possibly reflects a limited access of ABTS to the substrate binding site because of the hairpin presence. We also tested other mediators of different charge and hydrophobicity that could present better affinity for *Tt Lac* (ferrocenemethanol, ferrocenecarboxylic acid, DMP). None of them allowed higher MET currents to be observed.

Effect of Cu^{2+} on *Tt Lac* electrochemical behavior on Neg-CNT. One structural specificity of *Tt Lac* is the presence of the Met-rich hairpin. For CueO, such Met-rich domain organized in a helix was proposed to allow the enzyme to be involved in copper detoxification through the binding of exogenous copper atoms and subsequent oxidation of Cu^+ to the less toxic Cu^{2+} .⁴ The Met-rich helix was also proposed to cover the substrate binding site thus restricting access of bulky substrates like ABTS, while the bound copper would promote ET from the substrate to Cu T1.¹²

We confirmed in the present work the previously reported enhancement of the spectrophotometric activity of *Tt Lac* measured in solution in the presence of ABTS with increasing addition of Cu^{2+} (Figure S6).³ The K_M for ABTS was decreased to 1.6 mM in the presence of Cu^{2+} and the activity was enhanced *ca.* 3 times (Table S2). Whether the absence of direct ET process on Neg-CNT could be alleviated by addition of exogenous Cu^{2+} as occurring in solution is one fundamental issue to be investigated. Cupric salts were added in the NaAc buffer solution, and the electrochemical signal under O_2 was recorded with *Tt Lac* immobilized on Neg-CNT. A typical CV is given in Figure 5 for 500 μM Cu^{2+} concentration. A cathodic signal, with no anodic counterpart, is occurring on the first and following cycles with an onset potential close to +270 mV. This signal does not occur under N_2 or in the absence of Lac, and

it vanishes after addition of fluoride, known to inhibit O_2 catalytic reduction by MCOs, in the solution. A control experiment shows that Cu^{2+} in the absence of *Tt* Lac is reduced at a potential at least 150 mV lower on the Neg-CNT based electrode (Figure S7).

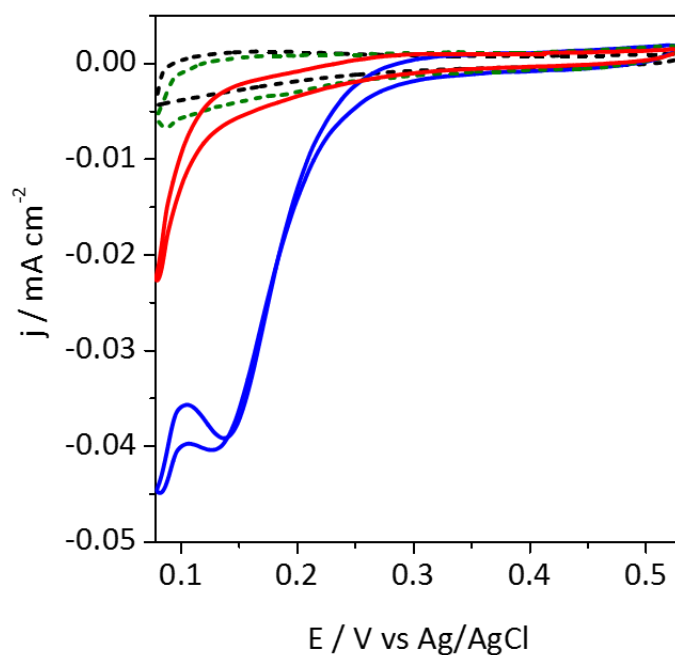


Figure 5: CVs under O_2 of *Tt* Lac adsorbed on Neg-CNT without (black dashed curve) or in the presence of $500 \mu\text{M}$ $CuSO_4$ (blue solid curve). CV under N_2 of *Tt* Lac adsorbed on Neg-CNT in the presence of $500 \mu\text{M}$ $CuSO_4$ is given as a green dashed curve. The red curve is obtained after 40 mM NaF addition in the oxygenated buffer containing $CuSO_4$. 0.1 M $NaAc$ buffer pH 5, scan rate 5 mV s^{-1} .

To get more insight in this new catalytic process, increasing additions of Cu^{2+} into the buffer electrolyte were realized with *Tt* Lac adsorbed on the Neg-CNT (Figure 6A).

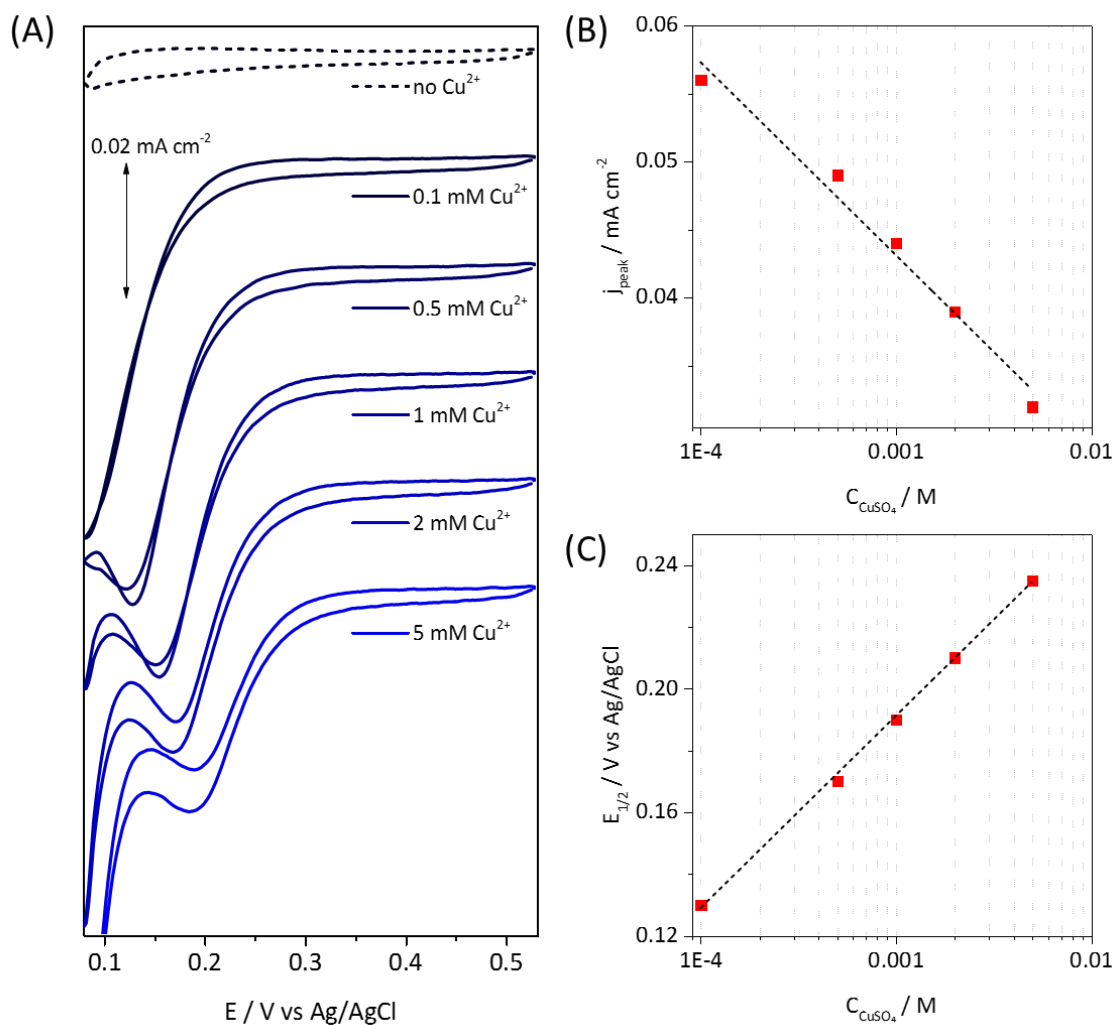


Figure 6: (A) CVs under O_2 with *Tt* Lac adsorbed on Neg-CNT in the presence of increasing CuSO_4 concentrations from zero to 5 mM. (B, C) Dependence of the half wave potential and peak current density on CuSO_4 concentration. 0.1 M NaAc buffer pH 5, scan rate 5 mV s^{-1} .

Within a concentration range from $100 \mu\text{M}$ to 5 mM Cu^{2+} , the typical Cu^{2+} -dependent catalytic wave appears with a half wave potential which is shifted anodic linearly with $\log[\text{Cu}^{2+}]$ with a slope of 62 mV (Figure 6C). For each Cu^{2+} concentration, the CV curve is characterized by a peak current, followed by the cathodic current increase in relation to the direct reduction of Cu^{2+} independent of the enzyme (Figure S7A). Within the current density range, there is no effect of the rotation rate on the shape of the catalytic wave nor on the magnitude of the peak current, which decreases linearly with $\log[\text{Cu}^{2+}]$ (Figure 6B). When excesses of EDTA or BCS

as Cu^{2+} and Cu^+ chelators respectively were added in the buffer solution containing Cu^{2+} , the Cu-related catalytic wave disappeared (Figure S8). As a control experiment, we also demonstrated that the Cu^{2+} -dependent catalytic wave is not linked to Cu associated to the His-tag on the protein. Actually, as shown in Figure S8C, the catalytic wave persisted even with the non His-tag protein. In conclusion, the Cu^{2+} -dependent catalytic signal is clearly associated to the availability of free non-complexed Cu^{2+} in solution.

Based on these experimental data, several hypotheses able to clarify the exact process behind Cu^{2+} -induced activation might be formulated: i) Cu^{2+} binding to *Tt* Lac lowers the electrostatic repulsion of the negative Cu T1 region allowing the enzyme to be re-orientated in a way more favorable for DET through Cu T1 center; ii) Cu^{2+} bound to *Tt* Lac forms a complex acting as a catalyst itself for oxygen reduction without participation of Cu T1/T2/T3 centers; iii) Cu^{2+} bound to *Tt* Lac participates into ET forming an additional electron relay between the electrode and Cu T1 (or Cu T2/T3); iv) the observed wave is related to the cuprous oxidase activity previously proposed for MCOs such as *Tt* Lac.

In the first hypothesis, Cu^{2+} ions would be acting as a shield of large negative charge near Cu T1 center allowing the latter to approach closer to the electrode surface for ET. Actually, Kano and coworkers found an increase in the catalytic performance when adding Ca^{2+} with *E. coli* CueO deposited on negative CNTs²⁵, which they attributed to the di-cations bridging the T1 Cu to the CNTs. To test this possibility, similar concentrations of Ca^{2+} , Zn^{2+} or Ni^{2+} were added in the buffer solution instead of Cu^{2+} . No effect on the electrochemical signal could be observed (Figure S9). Note also that these cations were shown to be useless in the activation of *Tt* Lac in solution.³

In the second hypothesis, we investigated the possibility of Cu^{2+} complexed by some *Tt* Lac residues to act as a molecular catalyst for oxygen reduction without Cu T1-T3 centers

involvement. Indeed, some copper complexes are known to act as catalysts for oxygen reduction, and we observed a catalytic process on Neg-CNT-modified electrode in the presence of Cu^{2+} but starting at potentials at least 0.15 V lower than the one in the presence of *Tt* Lac (Figure S7B). Alternatively, considering the low potential at which the Cu^{2+} -dependent catalytic process occurs, direct reduction of O_2 through the T2/T3 Cu site might occur, thus bypassing the intramolecular ET from Cu T1 to TNC. Such pathway was previously demonstrated using *Didymocrea* sp. J6 Lac immobilized on gold nanoparticles.⁴⁴ To rule out the two possibilities of non-enzymatic molecular copper complex implication and direct ET through the TNC, a Cu T1 deletant of *Tt* Lac was constructed in which Cys445 was replaced by Ala. In agreement with previous studies,^{45,46} this cysteine is essential for T1 copper binding and the purified mutant was white-colored due to the absence of Cu T1, and inactive. ICP and UV-Vis analyses showed that it still contains 2.3 atoms of Cu organized as T2/T3 center (Table S2, Figure S10A), and CD spectrum confirmed that the mutant mostly retained its secondary structure (Figure S10B). We thus conclude that the mutation was successful although the absence of Cu T1 partially impacted the protein folding. After adsorption of this mutant on Neg-CNT and addition of Cu^{2+} in solution, no catalysis could be observed (Figure 7), suggesting that the Cu^{2+} -dependent catalytic process proceeds necessarily through the laccase Cu T1 center and that no molecular Cu-complex is implicated in the catalysis.

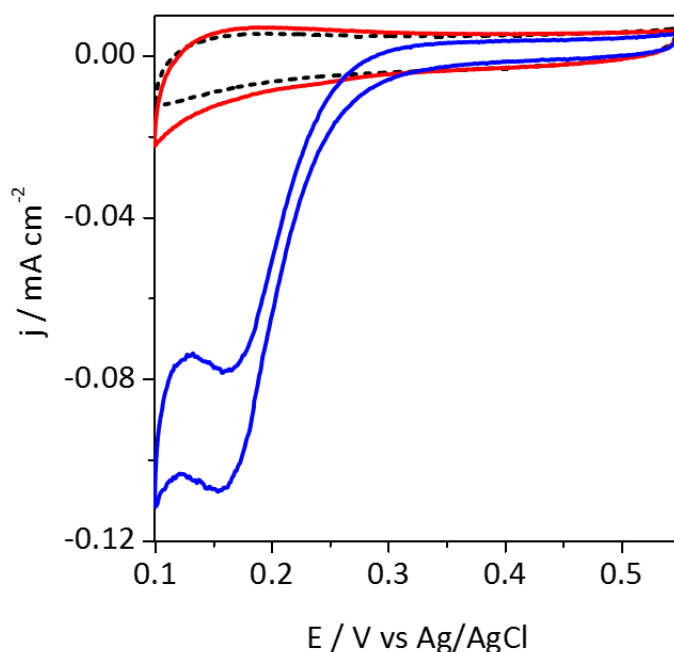
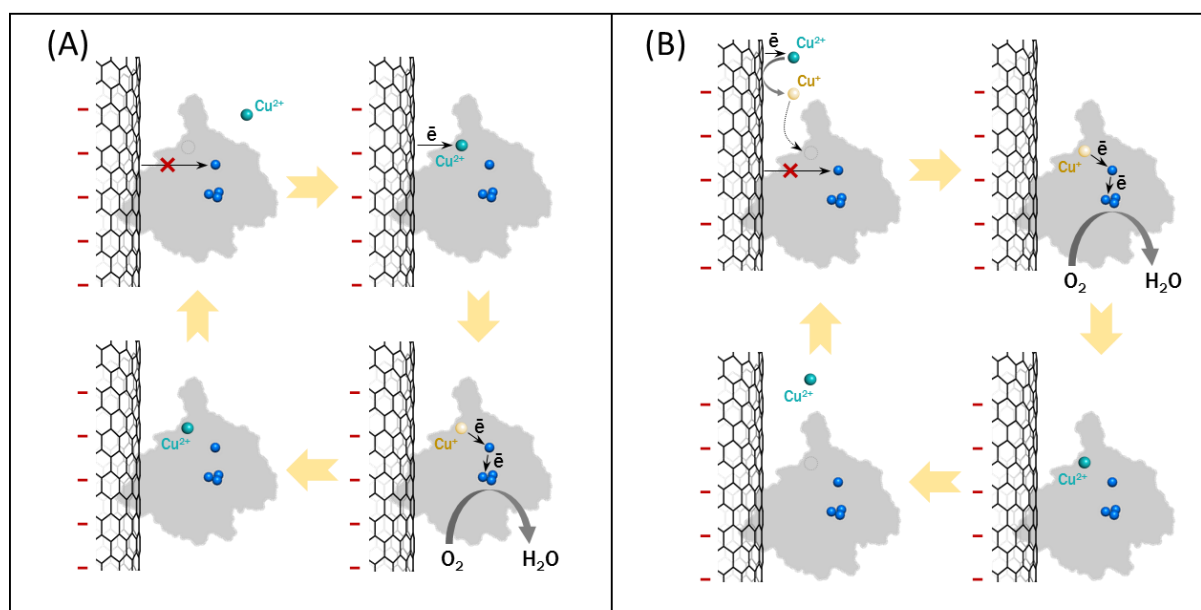


Figure 7: CVs of *Tt* Lac C445A adsorbed on Neg-CNT in the absence (black dashed line) and presence (red line) of 1 mM CuSO₄. The blue line represents the CV for Neg-CNT with *Tt* Lac WT in the presence of 1 mM CuSO₄. 0.1 M NaAc buffer pH 5, scan rate 5 mV s⁻¹, O₂ atmosphere.

Both two remaining hypothesis imply Cu²⁺/Cu⁺ binding at a coordination site close to the Cu T1 center allowing ET to it (Scheme 1A,B). In the case iii, the catalytic cycle starts with Cu²⁺ binding to this coordination site, yet with low affinity.¹³ Following this binding step, an additional relay is formed in the proximity of the electrode, bridging it with the Cu T1 center and enabling the reduction of O₂ through the newly formed ET pathway. Similar mechanism of copper action was suggested in previous publications studying *E. coli* CueO or *Tt* Lac activities in solution,¹³ but it has never been described in electrochemical studies. In the case iv the extremely small amounts of Cu⁺ formed at the electrode at potentials more than 200 mV higher than the formal Cu²⁺/Cu⁺ potential would be immediately bound by a high affinity coordination site in *Tt* Lac. The enzyme then exhibits its cuprous oxidase activity and oxidizes Cu⁺ to Cu²⁺

while transferring electrons to oxygen molecules through the classical T1-T2/T3 chain. The Cu^{2+} is released to the solution and is able to be reduced at the electrode again thus completing the catalytic cycle. The final result of both mechanisms would be ET from the electrode to oxygen by means of copper ions and the enzyme molecule, the difference being only the relative affinities of the coordination site for Cu^{2+} and Cu^+ and whether the first ET step happens to Cu-enzyme complex or not (Scheme 1).



Scheme 1. Proposed mechanisms of copper-induced catalytic wave formation on Neg-CNTs-Tt Lac: (A) copper – electron relay according to the hypothesis iii and (B) copper – substrate according to the hypothesis iv.

In a previous study relative to cuprous oxidase activity of CueO in solution, the authors fixed Cu^{2+} ion at the proposed coordination site by using MOPS, a buffer with low affinity to $\text{Cu}^{2+}/\text{Cu}^+$.¹³ We couldn't use MOPS for the desired pH-range, but we tested another buffer based on diethylpiperazine which is not able to form any complexes with transition metals due to steric hindrance.⁴⁷ Unlike the CueO work, we were unable to fix the Cu^{2+} at an additional coordination site whatever the buffer used. After electrode rinsing and transfer to a copper-free

buffer, the Cu-related catalytic wave vanishes (Figure S11). This suggests rather weak binding of the Cu^{2+} and tends to privilege the hypothesis iv as a more probable explanation of the observed electrocatalytic process.

What we observe therefore is the cuprous oxidase activity of *Tt* Lac initiated by substrate generation on the electrode. The fact that the catalytic wave onset is observed at potentials 150 mV more positive than the copper reduction on the bare electrode suggests a high affinity of *Tt* Lac for Cu^+ since only negligible amount of Cu^{2+} is reduced at this potential. A similar apparent shift of the mediated catalysis potential was observed recently for *M. thermophilum* cellobiose dehydrogenase and ferrocene monocarboxylic acid when the concentration of the latter was increasing.⁴⁸ From the extent of this shift, the authors concluded the catalytic concentration of the mediator necessary to sustain a given current. In our case, the precise analysis is not possible since $\text{Cu}^{2+}/\text{Cu}^+$ redox process is complicated by Cu^+ -disproportionation and complexation, but we can roughly estimate that *Tt* Lac starts to demonstrate its cuprous oxidase activity when Cu^+ concentration is in the nanomolar range (SI).

The validity of such pathway is further attested by the response analysis in the absence of oxygen (Figure S12). In these conditions, the catalytic wave is absent but a cathodic current increase is still observed with the increase of Cu^{2+} concentration, this time with an anodic counterpart (Figure S12B). The potential of the cathodic peak is in the agreement with the onset of the Cu-related catalytic wave and it demonstrates a similar shift with Cu^{2+} concentration (Figure 6). According to the hypothesis iv, the cathodic peak in the presence of enzyme can be explained by a facilitated reduction of Cu^{2+} into Cu^+ due to the further complexation of the latter with *Tt* Lac. The anodic counterpart appearing only in the anaerobic atmosphere thus corresponds to the inverse process in the conditions when the enzyme cannot perform catalytic oxidation of the bound Cu^+ . The more pronounced cathodic peak of the wild type *Tt* Lac in comparison with the anodic one should be explained by the contribution of the catalytic current

due to the presence of oxygen traces in the hydrophobic CNT-network. To eliminate any catalysis involvement, the C445A *Tt* Lac mutant, in which the Cu T1 is absent (Figure 7), was studied in the absence of O₂ with increasing Cu²⁺ concentrations. The Cu⁺ binding is still possible for such mutant, and CV peaks similar to the WT appeared in the anaerobic conditions (Figure S12C). The cathodic peak is less pronounced and its charge equals to the anodic one due to the absence of catalysis implication. The presence of these high potential Cu-related peaks for both *Tt* Lac WT and C445A mutant confirms the existence of a high affinity Cu⁺ binding site for this enzyme.

Another feature of the catalytic wave, which resembles to an inactivation/activation process, may be attributed to an inhibition process induced by Cu⁺ produced in excess on the electrode surface at low potentials. This type of inhibition was previously observed with other enzymes immobilized on electrodes. As illustrations, H⁺ reduction by hydrogenases was inhibited by H₂,⁴⁹ the reduction product, or nitrate reduction by nitrate oxidase was inhibited by nitrate,⁵⁰ leading in both cases to similar electrochemical signal shape as we have recorded in the presence of Cu²⁺ in this work. Besides, the inhibition by Cu⁺ concentrations higher than 0.1 mM was reported earlier for CueO.⁹

ET pathways within *Tt* Lac immobilized on Pos-CNTs. The next question is whether Cu²⁺ addition may also affect the DET signal obtained when *Tt* Lac is immobilized on Pos-CNT. Increasing Cu²⁺ amounts were thus added in the buffer solution and the CVs were run under O₂ (Figure 8).

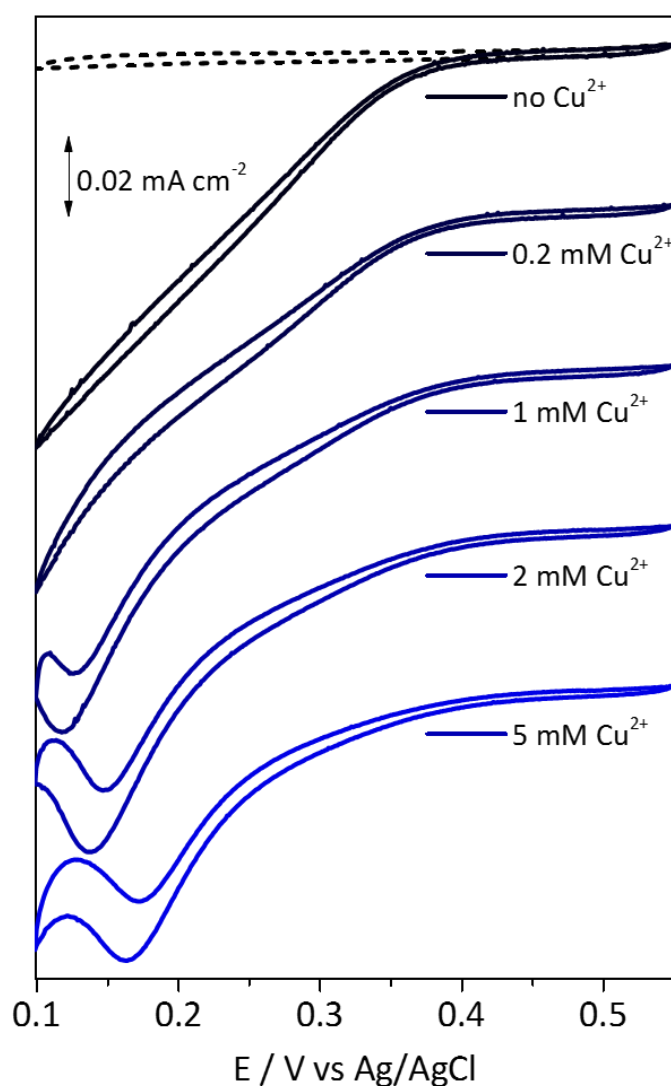
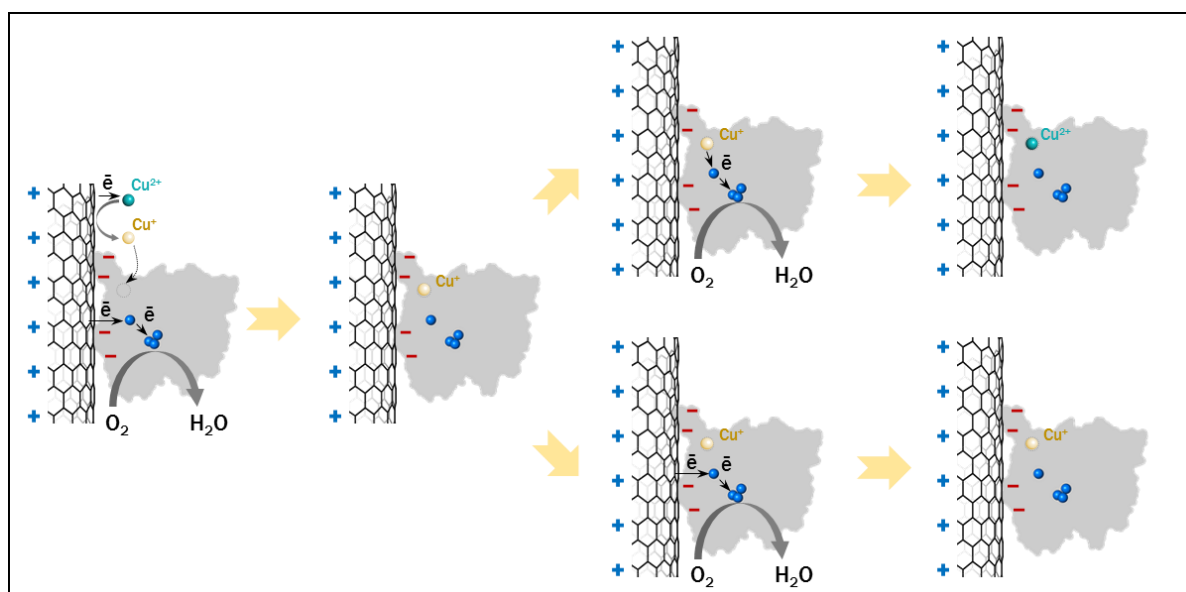


Figure 8: CV responses under O_2 by *Tt* Lac adsorbed on Pos-CNT with increasing concentrations of $CuSO_4$ from 0 to 5 mM. Dashed curve represents the same electrode in the absence of $CuSO_4$ under N_2 . 0.1 M NaAc buffer pH 5, scan rate 5 mV s^{-1} .

Starting from the DET signal for O_2 reduction by *Tt* Lac adsorbed on Pos-CNT, a decrease of the DET catalytic current is observed with increasing Cu^{2+} concentrations, especially visible at higher potentials. In the same time, the Cu^{2+} -dependent catalytic peak appears, similar to the one observed on Neg-CNT, also decreasing and shifting in potential with increasing Cu^{2+} concentrations. As a control, Ca^{2+} addition into the solution up to 5 mM has no effect on the DET process (Figure S13). When transferring the Pos-CNT-*Tt* Lac bioelectrode in a Cu^{2+} -free

buffer, not only the Cu^{2+} -dependent catalytic wave disappeared, but the DET signal was recovered (Figure S14). To explain the apparent competition between DET and Cu-related processes observed for *Tt* Lac on Pos-CNT, one should recall that in DET mode the electrons are transferred directly from the electrode to the T1 Cu center. In the presence of Cu^{2+} , cuprous oxidase activity can take place, and Cu^+ formed on the electrode can bind to the enzyme and also transfer electrons to the T1 center thus creating an alternative pathway competing with DET (Scheme 2). This observation may explain the decrease of the DET-current with Cu^{2+} addition and concomitant increase of the Cu-related wave. On the other hand, we don't expect 100% of adsorbed enzymes to be in DET orientation.⁵¹ These enzymes adsorbed in the orientation not favorable to DET process may still contribute to the cuprous oxidase activity since Cu^+ formed on the electrode can freely diffuse giving raise to the characteristic Cu-related catalytic wave.



Scheme 2. Proposed mechanism of copper-induced catalytic wave change on Pos-CNTs-*Tt* Lac.

Involvement of the Met-rich domain in the electrocatalysis. Now that we ascribed the appearance of the electrochemical wave upon copper addition to cuprous oxidase activity of *Tt* Lac, the exact position of Cu-binding remains to be found. It was suggested that Met-rich regions of proteins are involved in metal binding and transport.^{52,53} In this aspect, the Met-rich hairpin functionally resembles the Met-rich helix of *E.coli* CueO. If the Cu²⁺-dependent catalytic process is linked to the Met-rich hairpin of *Tt* Lac, such catalytic process should not occur in a multicopper oxidase which does not contain any Met-rich domain. *B. pumilus* BOD is an excellent control for that aim, because it does not yield any DET on Neg-CNT as *Tt* Lac. As shown in Figure S15, the addition of Cu²⁺ up to 20 mM does not allow the Cu²⁺-dependent catalytic signal to be observed when using *B. pumilus* BOD.

We therefore constructed a deletant of *Tt* Lac, named Δ -hairpin Lac, where we deleted a part of the sequence between residues A292 and G308 that constitutes the hairpin and contains 6 methionines. The Δ -hairpin Lac conserved 82% activity compared to the WT and was still able to be activated by copper addition in the ABTS solution assay. Its K_M was insignificantly increased compared to WT falling within the range of the experimental error (Table S2). These results drastically differ from those obtained with the Met-rich helix deletant of CueO which showed a 40-fold increase of ABTS-oxidizing activity and disappearance of copper activation in solution.¹⁹ We therefore conclude that, unlike in the case of CueO helix, the hairpin of *Tt* Lac doesn't present a steric hindrance for the ABTS binding and the low ABTS-oxidizing activity of *Tt* Lac must be explained by other reasons, i.e. low affinity. Interestingly, MD simulations of *Tt* Lac and analogous hairpin-deletant earlier demonstrated a similar manner of ABTS docking to both molecules despite hairpin absence thus confirming our experimental observations.^{54,55}

In agreement with the solution assay, the Δ -hairpin Lac behaved similarly to the wild type when immobilized on Neg-CNTs or Pos-CNTs (Figure S16). On Neg-CNTs no DET process could be observed, and a catalytic wave similar to the WT was obtained in the presence of Cu^{2+} . The absence of DET is understandable because the charge in the vicinity of Cu T1 remains negative in Δ -hairpin Lac. However, the persistence of the Cu^{2+} -dependant catalytic process despite the deletion of the Met-rich hairpin confirms that the hairpin domain is not required for *Tt* Lac copper-activated catalytic process.

Actually, in CueO related studies, it was underlined that besides Cu binding sites in the Met-rich helix another sCu binding site is located beyond the helix and formed by M355, D360, D439, and M441 residues. It is situated along a distance of 7.5 Å to the Cu T1 and linked to it through a hydrogen-bond that might be involved in an ET pathway.¹¹ Such site wasn't previously identified in *Tt* Lac.³ Our sequence alignment suggests however that a similar Cu-binding site cannot be excluded taking into account that at least three from four residues of *Tt* Lac (D353, D390, M391) are well aligned with the Cu-binding residues of CueO (Figures S17 and S18). These three residues were not altered by the hairpin deletion (Figure S17) which may explain the conservation of the copper activation process in this mutant.

CONCLUDING REMARKS

We demonstrated that thanks to a particular surface charge distribution and using different CNTs, *Tt* Lac can be adsorbed on the electrode surface in an orientation either favoring DET through T1 or virtually precluding it. Inspired by a related MCO, *E.coli* CueO, we used this feature to study electrochemically the influence of Cu^{2+} on the activity of *Tt* Lac. The electrode with *Tt* Lac adsorbed in the no-DET orientation exhibits a low-potential cathodic catalytic wave upon Cu^{2+} addition into the electrochemical cell. This wave was not reported earlier in any studies on either *E. coli* CueO or *Tt* Lac. We ascribe it to a cuprous oxidase activity of *Tt* Lac emerging due to nanomolar amounts of Cu^+ being produced directly on the electrode. The same

wave appears and gradually suppresses the direct ET through Cu T1 when *Tt* Lac is adsorbed in the favorable orientation. We rely on these data to propose the mechanism of copper binding and oxidation by *Tt* Lac with electrons transferred to Cu T1.

The cuprous oxidase activity of *Tt* Lac is apparently responsible for the enhancement of the spectrophotometric activity for ABTS oxidation observed earlier in solution assay in the presence of increasing amounts of Cu^{2+} .³ This phenomenon should be discussed apart since there is no Cu^+ present in the assay, contrary to the electrochemical system where it is generated on the electrode. In the case of *E. coli* CueO, such enhancement was shown to be caused by the occupation of sCu site by a copper atom required for phenol oxidase activity. This additional copper atom would mediate ET between buried Cu T1 and the organic substrate. Apparently, the same behavior is valid for *Tt* Lac in the cuvette where the presence of labile Cu^{2+} at hypothetical sCu site allows to enhance ABTS oxidizing activity. We speculate that higher specificity of this site for Cu^+ than Cu^{2+} leads to the increase of redox potential of $\text{sCu}^{2+}/\text{sCu}^+$ couple, which becomes able to withdraw electrons from ABTS and pass them further to Cu T1.

In the solution assay, it cannot be distinguished whether the increase of oxidized ABTS concentration reflecting enzyme activity is related to electrons transferred first from ABTS to sCu or to Cu T1. We propose that using protein voltammetry we are able to discriminate whether electrons enter the enzyme directly from the electrode or by means of exogenous copper. Once exogenous copper is present, it opens a possibility for the new pathway via binding and oxidizing Cu^+ at sCu-site. Electrochemically, the appearance of this new electron pathway is translated into the change of reduction potential and decrease of DET current, if any, through Cu T1. Another advantage of voltammetry is the fact that small amounts of Cu^+ can be produced in a controllable manner at the electrode in the vicinity of enzyme molecules and react with them before entering into Fenton or disproportionation reactions. We thus propose electrochemistry as a powerful tool to study a cuprous oxidase activity of MCOs.

As such, the Cu-related mechanism of *Tt* Lac is homologous to the cuprous oxidase activity of *E.coli* CueO, suggesting that both enzymes might fulfill similar physiological roles of copper detoxification *in vivo*. However, unlike *E.coli* CueO mutant with deleted Met-rich region, the removal of the corresponding Met-rich hairpin of *Tt* Lac did not lead to an enhanced phenol oxidase activity while copper activation persisted. This suggests certain divergence in the behavior of these two enzymes, notably non-involvement of Met-rich hairpin of *Tt* Lac in copper binding and oxidation. We anticipate that future site-directed mutagenesis will allow to elucidate the details and differences of their mechanisms.

SUPPORTING INFORMATION

Protease TEV purification; SPR, ellipsometry, CD spectroscopy, ICP-OES methods description; calculation of *Tt* Lac affinity for Cu⁺; loading of *Tt* Lac on SAM-modified gold electrodes; XPS spectra of CNTs; CVs of *Tt* Lac in anaerobic conditions; CVs of *Tt* Lac at different rotation speeds; CVs of His-tag-cleaved *Tt* Lac, CVs of *Bp* BOD before and after Cu²⁺ addition; enhancement of *Tt* Lac activity as a function of Cu²⁺ concentration; CVs of different concentrations of Cu²⁺ at Neg-CNT in the presence and absence of *Tt* Lac and O₂; effect of chelators and other cations (Ca²⁺, Zn²⁺, Ni²⁺); UV-Vis and CD spectrum of C445A mutant; CVs in DEPP buffer and CVs of electrode transfer to a copper-free buffer; CVs of *Tt* Lac WT and C445A mutant on Neg-CNTs in anaerobic conditions and in the presence of Cu²⁺; CVs of the Δ -hairpin mutant; sequences alignment and structures superposition of *Tt* Lac and *E.coli* CueO; oligonucleotides used; kinetic and thermodynamic parameters of *Tt* Lac and mutants.

ACKNOWLEDGMENT

This work was supported by ANR (ENZYMOR-ANR-16-CE05- 0024) and Aix-Marseille University for V.P. Hitaishi's funding. The authors thank Emna Abdeljaoued, Xie Wang,

Pascale Infossi and Proteomic Analysis Center (IMM, CNRS, Marseille) for experimental assistance, Dr Ling Peng from CINAM (Marseille) for access to zetasizer facility, Dr N. Mano (CRPP, Bordeaux) for the kind gift of *Bp* BOD, Dr Marie-Thérèse Giudici-Ortoni for fruitful discussions and Dr Anne de Poulpiquet for critical reading of the manuscript.

REFERENCES

- (1) Mano, N.; De Poulpiquet, A. O₂ Reduction in Enzymatic Biofuel Cells. *Chem. Rev.* **2018**, *118* (5), 2392–2468. <https://doi.org/10.1021/acs.chemrev.7b00220>.
- (2) Jones, S. M.; Solomon, E. I. Electron Transfer and Reaction Mechanism of Laccases. *Cell. Mol. Life Sci.* **2015**, *72* (5), 869–883. <https://doi.org/10.1007/s00018-014-1826-6>.
- (3) Miyazaki, K. A Hyperthermophilic Laccase from *Thermus Thermophilus* HB27. *Extremophiles* **2005**, *9* (6), 415–425. <https://doi.org/10.1007/s00792-005-0458-z>.
- (4) Serrano-Posada, H.; Valderrama, B.; Stojanoff, V.; Rudiño-Piñera, E. Thermostable Multicopper Oxidase from *Thermus Thermophilus* HB27: Crystallization and Preliminary X-Ray Diffraction Analysis of Apo and Holo Forms. *Acta Crystallogr. Sect. F. Struct. Biol. Cryst. Commun.* **2011**, *67* (Pt 12), 1595–1598. <https://doi.org/10.1107/S174430911103805X>.
- (5) Serrano-Posada, H.; Centeno-Leija, S.; Rojas-Trejo, S. P.; Rodríguez-Almazán, C.; Stojanoff, V.; Rudiño-Piñera, E. X-Ray-Induced Catalytic Active-Site Reduction of a Multicopper Oxidase: Structural Insights into the Proton-Relay Mechanism and O₂-Reduction States. *Acta Crystallogr. Sect. D Biol. Crystallogr.* **2015**, *71*, 2396–2411. <https://doi.org/10.1107/S1399004715018714>.
- (6) Rensing, C.; Grass, G. Escherichia Coli Mechanisms of Copper Homeostasis in a Changing Environment. *FEMS Microbiol. Rev.* **2003**, *27* (2–3), 197–213. [https://doi.org/10.1016/S0168-6445\(03\)00049-4](https://doi.org/10.1016/S0168-6445(03)00049-4).
- (7) Tree, J. J.; Kidd, S. P.; Jennings, M. P.; McEwan, A. G. Copper Sensitivity of CueO Mutants of Escherichia Coli K-12 and the Biochemical Suppression of This Phenotype. *Biochem. Biophys. Res. Commun.* **2005**, *328* (4), 1205–1210. <https://doi.org/10.1016/J.BBRC.2005.01.084>.
- (8) Rensing, C.; McDevitt, S. F. The Copper Metallome in Prokaryotic Cells. In *Metallomics and the Cell*; Banci, L., Ed.; Metal Ions in Life Sciences; Springer Netherlands: Dordrecht, 2013; Vol. 12, pp 417–450. <https://doi.org/10.1007/978-94-007-5561-1>.
- (9) Kataoka, K.; Komori, H.; Ueki, Y.; Konno, Y.; Kamitaka, Y.; Kurose, S.; Tsujimura, S.; Higuchi, Y.; Kano, K.; Seo, D.; Sakurai, T. Structure and Function of the Engineered Multicopper Oxidase CueO from Escherichia Coli-Deletion of the Methionine-Rich Helical Region Covering the Substrate-Binding Site. *J. Mol. Biol.* **2007**, *373* (1), 141–152. <https://doi.org/10.1016/j.jmb.2007.07.041>.

- (10) Kurose, S.; Kataoka, K.; Otsuka, K.; Tsujino, Y.; Sakurai, T. Promotion of Laccase Activities of *Escherichia Coli* Cuprous Oxidase, CueO by Deleting the Segment Covering the Substrate Binding Site. *Chem. Lett.* **2007**, *36* (2), 232–233. <https://doi.org/10.1246/cl.2007.232>.
- (11) Roberts, S. A.; Wildner, G. F.; Grass, G.; Weichsel, A.; Ambrus, A.; Rensing, C.; Montfort, W. R. A Labile Regulatory Copper Ion Lies near the T1 Copper Site in the Multicopper Oxidase CueO. *J. Biol. Chem.* **2003**, *278* (34), 31958–31963. <https://doi.org/10.1074/jbc.M302963200>.
- (12) Singh, S. K.; Roberts, S. A.; McDevitt, S. F.; Weichsel, A.; Wildner, G. F.; Grass, G. B.; Rensing, C.; Montfort, W. R. Crystal Structures of Multicopper Oxidase CueO Bound to Copper(I) and Silver(I): Functional Role of a Methionine-Rich Sequence. *J. Biol. Chem.* **2011**, *286* (43), 37849–37857. <https://doi.org/10.1074/jbc.M111.293589>.
- (13) Djoko, K. Y.; Chong, L. X.; Wedd, A. G.; Xiao, Z. Reaction Mechanisms of the Multicopper Oxidase CueO from *Escherichia Coli* Support Its Functional Role as a Cuprous Oxidase. *J. Am. Chem. Soc.* **2010**, *132* (6), 2005–2015. <https://doi.org/10.1021/ja9091903>.
- (14) Cortes, L.; Wedd, A. G.; Xiao, Z. The Functional Roles of the Three Copper Sites Associated with the Methionine-Rich Insert in the Multicopper Oxidase CueO from *E. Coli*. *Metallomics* **2015**, *7* (5), 776–785. <https://doi.org/10.1039/C5MT00001G>.
- (15) Page, C. C.; Moser, C. C.; Chen, X.; Dutton, P. L. Natural Engineering Principles of Electron Tunnelling in Biological Oxidation-Reduction. *Nature* **1999**, *402* (6757), 47–52. <https://doi.org/10.1038/46972>.
- (16) Miura, Y.; Tsujimura, S.; Kamitaka, Y.; Kurose, S.; Kataoka, K.; Sakurai, T.; Kano, K. Bioelectrocatalytic Reduction of O₂ Catalyzed by CueO from *Escherichia Coli* Adsorbed on a Highly Oriented Pyrolytic Graphite Electrode. *Chem. Lett.* **2007**, *36* (1), 132–133. <https://doi.org/10.1246/cl.2007.132>.
- (17) Miura, Y.; Tsujimura, S.; Kurose, S.; Kamitaka, Y.; Kataoka, K.; Sakurai, T.; Kano, K. Direct Electrochemistry of CueO and Its Mutants at Residues to and Near Type I Cu for Oxygen-Reducing Biocathode. *Fuel Cells* **2009**, *9* (1), 70–78. <https://doi.org/10.1002/fuce.200800027>.
- (18) Kontani, R.; Tsujimura, S.; Kano, K. Air Diffusion Biocathode with CueO as Electrocatalyst Adsorbed on Carbon Particle-Modified Electrodes. *Bioelectrochemistry* **2009**, *76* (1–2), 10–13. <https://doi.org/10.1016/J.BIOELECTCHEM.2009.02.009>.
- (19) Kataoka, K.; Kogi, H.; Tsujimura, S.; Sakurai, T. Modifications of Laccase Activities of Copper Efflux Oxidase, CueO by Synergistic Mutations in the First and Second Coordination Spheres of the Type I Copper Center. *Biochem. Biophys. Res. Commun.* **2013**, *431* (3), 393–397. <https://doi.org/10.1016/J.BBRC.2013.01.040>.
- (20) Sugimoto, Y.; Kitazumi, Y.; Tsujimura, S.; Shirai, O.; Yamamoto, M.; Kano, K. Electrostatic Interaction between an Enzyme and Electrodes in the Electric Double Layer Examined in a View of Direct Electron Transfer-Type Bioelectrocatalysis. *Biosens. Bioelectron.* **2015**, *63*, 138–144. <https://doi.org/10.1016/j.bios.2014.07.025>.
- (21) Schlesinger, O.; Pasi, M.; Dandela, R.; Meijler, M. M.; Alfonta, L. Electron Transfer

- Rate Analysis of a Site-Specifically Wired Copper Oxidase. *Phys. Chem. Chem. Phys.* **2018**, *20*, 6159–6166. <https://doi.org/10.1039/C8CP00041G>.
- (22) Zhang, L.; Cui, H.; Zou, Z.; Garakani, T. M.; Novoa-Henriquez, C.; Jooyeh, B.; Schwaneberg, U. Directed Evolution of a Bacterial Laccase (CueO) for Enzymatic Biofuel Cells. *Angew. Chemie - Int. Ed.* **2019**, *58* (14), 4562–4565. <https://doi.org/10.1002/anie.201814069>.
- (23) Climent, V.; Fu, Y.; Chumillas, S.; Maestro, B.; Li, J.-F.; Kuzume, A.; Keller, S.; Wandlowski, T. Probing the Electrocatalytic Oxygen Reduction Reaction Reactivity of Immobilized Multicopper Oxidase CueO. *J. Phys. Chem. C* **2014**, *118* (29), 15754–15765. <https://doi.org/10.1021/jp5034382>.
- (24) Chumillas, S.; Maestro, B.; Feliu, J. M.; Climent, V. Comprehensive Study of the Enzymatic Catalysis of the Electrochemical Oxygen Reduction Reaction (ORR) by Immobilized Copper Efflux Oxidase (CueO) From Escherichia Coli. *Front. Chem.* **2018**, *6*, 358. <https://doi.org/10.3389/fchem.2018.00358>.
- (25) Xia, H.; Kitazumi, Y.; Shirai, O.; Ozawa, H.; Onizuka, M.; Komukai, T.; Kano, K. Factors Affecting the Interaction between Carbon Nanotubes and Redox Enzymes in Direct Electron Transfer-Type Bioelectrocatalysis. *Bioelectrochemistry* **2017**, *118*, 70–74. <https://doi.org/10.1016/J.BIOELECTCHEM.2017.07.003>.
- (26) Liu, X.; Gillespie, M.; Ozel, A. D.; Dikici, E.; Daunert, S.; Bachas, L. G. Electrochemical Properties and Temperature Dependence of a Recombinant Laccase from Thermus Thermophilus. *Anal. Bioanal. Chem.* **2011**, *399* (1), 361–366. <https://doi.org/10.1007/s00216-010-4345-9>.
- (27) Agbo, P.; Heath, J. R.; Gray, H. B. Catalysis of Dioxygen Reduction by Thermus Thermophilus Strain Hb27 Laccase on Ketjen Black Electrodes. *J. Phys. Chem. B* **2013**, *117* (2), 527–534. <https://doi.org/10.1021/jp309759g>.
- (28) Agbo, P.; Heath, J. R.; Gray, H. B. Modeling Dioxygen Reduction at Multicopper Oxidase Cathodes. *J. Am. Chem. Soc.* **2014**, *136* (39), 13882–13887. <https://doi.org/10.1021/ja5077519>.
- (29) Gounel, S.; Rouhana, J.; Stines-Chaumeil, C.; Cadet, M.; Mano, N. Increasing the Catalytic Activity of Bilirubin Oxidase from Bacillus Pumilus: Importance of Host Strain and Chaperones Proteins. *J. Biotechnol.* **2016**, *230*, 19–25. <https://doi.org/10.1016/j.jbiotec.2016.04.035>.
- (30) Jeong, J.-Y.; Yim, H.-S.; Ryu, J.-Y.; Lee, H. S.; Lee, J.-H.; Seen, D.-S.; Kang, S. G. One-Step Sequence- and Ligation-Independent Cloning as a Rapid and Versatile Cloning Method for Functional Genomics Studies. *Appl. Environ. Microbiol.* **2012**, *78* (15), 5440–5443. <https://doi.org/10.1128/AEM.00844-12>.
- (31) Durão, P.; Chen, Z.; Fernandes, A. T.; Hildebrandt, P.; Murgida, D. H.; Todorovic, S.; Pereira, M. M.; Melo, E. P.; Martins, L. O. Copper Incorporation into Recombinant CotA Laccase from Bacillus Subtilis: Characterization of Fully Copper Loaded Enzymes. *JBIC J. Biol. Inorg. Chem.* **2008**, *13* (2), 183–193. <https://doi.org/10.1007/s00775-007-0312-0>.
- (32) Hitaishi, V. P.; Mazurenko, I.; Harb, M.; Clément, R.; Taris, M.; Castano, S.; Duché, D.;

- Lecomte, S.; Ilbert, M.; de Poulpiquet, A.; Lojou, E. Electrostatic-Driven Activity, Loading, Dynamics, and Stability of a Redox Enzyme on Functionalized-Gold Electrodes for Bioelectrocatalysis. *ACS Catal.* **2018**, 12004–12014. <https://doi.org/10.1021/acscatal.8b03443>.
- (33) Mazurenko, I.; Monsalve, K.; Rouhana, J.; Parent, P.; Laffon, C.; Goff, A. Le; Szunerits, S.; Boukherroub, R.; Giudici-Ortoni, M.-T.; Mano, N.; Lojou, E. How the Intricate Interactions between Carbon Nanotubes and Two Bilirubin Oxidases Control Direct and Mediated O₂ Reduction. *ACS Appl. Mater. Interfaces* **2016**, 8 (35), 23074–23085. <https://doi.org/10.1021/acsami.6b07355>.
- (34) Dolinsky, T. J.; Nielsen, J. E.; McCammon, J. A.; Baker, N. A. PDB2PQR: An Automated Pipeline for the Setup of Poisson-Boltzmann Electrostatics Calculations. *Nucleic Acids Res.* **2004**, 32 (Web Server issue), W665-7. <https://doi.org/10.1093/nar/gkh381>.
- (35) Søndergaard, C. R.; Olsson, M. H. M.; Rostkowski, M.; Jensen, J. H. Improved Treatment of Ligands and Coupling Effects in Empirical Calculation and Rationalization of pK_a Values. *J. Chem. Theory Comput.* **2011**, 7 (7), 2284–2295. <https://doi.org/10.1021/ct200133y>.
- (36) Felder, C. E.; Prilusky, J.; Silman, I.; Sussman, J. L. A Server and Database for Dipole Moments of Proteins. *Nucleic Acids Res.* **2007**, 35 (Web Server issue), W512-21. <https://doi.org/10.1093/nar/gkm307>.
- (37) Ashkenazy, H.; Erez, E.; Martz, E.; Pupko, T.; Ben-Tal, N. ConSurf 2010: Calculating Evolutionary Conservation in Sequence and Structure of Proteins and Nucleic Acids. *Nucleic Acids Res.* **2010**, 38 (Web Server), W529–W533. <https://doi.org/10.1093/nar/gkq399>.
- (38) Kelley, L. A.; Mezulis, S.; Yates, C. M.; Wass, M. N.; Sternberg, M. J. E. The Phyre2 Web Portal for Protein Modeling, Prediction and Analysis. *Nat. Protoc.* **2015**, 10 (6), 845–858. <https://doi.org/10.1038/nprot.2015.053>.
- (39) Madeira, F.; Park, Y. mi; Lee, J.; Buso, N.; Gur, T.; Madhusoodanan, N.; Basutkar, P.; Tivey, A. R. N.; Potter, S. C.; Finn, R. D.; Lopez, R. The EMBL-EBI Search and Sequence Analysis Tools APIs in 2019. *Nucleic Acids Res.* **2019**, 47 (W1), W636–W641. <https://doi.org/10.1093/nar/gkz268>.
- (40) Robert, X.; Gouet, P. Deciphering Key Features in Protein Structures with the New ENDscript Server. *Nucleic Acids Res.* **2014**, 42 (W1), W320–W324. <https://doi.org/10.1093/nar/gku316>.
- (41) Xu, F.; Palmer, A. E.; Yaver, D. S.; Berka, R. M.; Gambetta, G. A.; Brown, S. H.; Solomon, E. I. Targeted Mutations in a *Trametes Villosa* Laccase. *J. Biol. Chem.* **1999**, 274 (18), 12372–12375. <https://doi.org/10.1074/jbc.274.18.12372>.
- (42) Scherbahn, V.; Putze, M. T.; Dietzel, B.; Heinlein, T.; Schneider, J. J.; Lisdat, F. Biofuel Cells Based on Direct Enzyme-Electrode Contacts Using PQQ-Dependent Glucose Dehydrogenase/Bilirubin Oxidase and Modified Carbon Nanotube Materials. *Biosens. Bioelectron.* **2014**, 61, 631–638. <https://doi.org/10.1016/j.bios.2014.05.027>.
- (43) Mano, N. Features and Applications of Bilirubin Oxidases. *Appl. Microbiol. Biotechnol.*

- 2012**, 96 (2), 301–307. <https://doi.org/10.1007/s00253-012-4312-9>.
- (44) Dagys, M.; Laurynėnas, A.; Ratautas, D.; Kulys, J.; Vidžiūnaitė, R.; Talaikis, M.; Niaura, G.; Marcinkevičienė, L.; Meškys, R.; Shleev, S. Oxygen Electroreduction Catalysed by Laccase Wired to Gold Nanoparticles via the Trinuclear Copper Cluster. *Energy Environ. Sci.* **2017**, 10 (2), 498–502. <https://doi.org/10.1039/C6EE02232D>.
- (45) Zeng, J.; Geng, M.; Liu, Y.; Xia, L.; Liu, J.; Qiu, G. The Sulfhydryl Group of Cys138 of Rusticyanin from *Acidithiobacillus Ferrooxidans* Is Crucial for Copper Binding. *Biochim. Biophys. Acta - Proteins Proteomics* **2007**, 1774 (4), 519–525. <https://doi.org/10.1016/j.bbapap.2007.02.008>.
- (46) Roger, M.; Sciara, G.; Biaso, F.; Lojou, E.; Wang, X.; Bauzan, M.; Giudici-Ortoni, M.-T.; Vila, A. J.; Ilbert, M. Impact of Copper Ligand Mutations on a Cupredoxin with a Green Copper Center. *Biochim. Biophys. Acta - Bioenerg.* **2017**, 1858 (5), 351–359. <https://doi.org/10.1016/j.bbabi.2017.02.007>.
- (47) Kandegedara, A.; Rorabacher, D. B. Noncomplexing Tertiary Amines as “better” Buffers Covering the Range of PH 3-11. Temperature Dependence of Their Acid Dissociation Constants. *Anal. Chem.* **1999**, 71 (15), 3140–3144. <https://doi.org/10.1021/ac9902594>.
- (48) Meneghello, M.; Al-Lolage, F. A.; Ma, S.; Ludwig, R.; Bartlett, P. N. Studying Direct Electron Transfer by Site-Directed Immobilization of Cellobiose Dehydrogenase. *ChemElectroChem* **2019**, 6 (3), 700–713. <https://doi.org/10.1002/celec.201801503>.
- (49) Fourmond, V.; Baffert, C.; Sybirna, K.; Dementin, S.; Abou-Hamdan, A.; Meynial-Salles, I.; Soucaille, P.; Bottin, H.; Léger, C. The Mechanism of Inhibition by H₂ of H₂-Evolution by Hydrogenases. *Chem. Commun.* **2013**, 49 (61), 6840. <https://doi.org/10.1039/c3cc43297a>.
- (50) Jacques, J. G. J.; Burlat, B.; Arnoux, P.; Sabaty, M.; Guigliarelli, B.; Léger, C.; Pignol, D.; Fourmond, V. Kinetics of Substrate Inhibition of Periplasmic Nitrate Reductase. *Biochim. Biophys. Acta - Bioenerg.* **2014**, 1837 (10), 1801–1809. <https://doi.org/10.1016/J.BBABIO.2014.05.357>.
- (51) Mazurenko, I.; Monsalve, K.; Infossi, P.; Giudici-Ortoni, M.-T.; Topin, F.; Mano, N.; Lojou, E. Impact of Substrate Diffusion and Enzyme Distribution in 3D-Porous Electrodes: A Combined Electrochemical and Modelling Study of a Thermostable H₂/O₂ Enzymatic Fuel Cell. *Energy Environ. Sci.* **2017**, 10, 1966–1982. <https://doi.org/10.1039/C7EE01830D>.
- (52) Xue, Y.; Davis, A. V.; Balakrishnan, G.; Stasser, J. P.; Staehlin, B. M.; Focia, P.; Spiro, T. G.; Penner-Hahn, J. E.; O’Halloran, T. V. Cu(I) Recognition via Cation- π and Methionine Interactions in CusF. *Nat. Chem. Biol.* **2008**, 4 (2), 107–109. <https://doi.org/10.1038/nchembio.2007.57>.
- (53) Doerrer, L. H. Cu in Biology: Unleashed by O₂ and Now Irreplaceable. *Inorganica Chim. Acta* **2018**, 481, 4–24. <https://doi.org/10.1016/j.ica.2017.11.051>.
- (54) Bello, M.; Valderrama, B.; Serrano-Posada, H.; Rudiño-Piñera, E. Molecular Dynamics of a Thermostable Multicopper Oxidase from *Thermus Thermophilus* HB27: Structural Differences between the Apo and Holo Forms. *PLoS One* **2012**, 7 (7), e40700.

<https://doi.org/10.1371/journal.pone.0040700>.

- (55) Bello, M.; Correa-Basurto, J.; Rudiño-Piñera, E. Simulation of the Cavity-Binding Site of Three Bacterial Multicopper Oxidases upon Complex Stabilization: Interactional Profile and Electron Transference Pathways. *J. Biomol. Struct. Dyn.* **2014**, *32* (8), 1303–1317. <https://doi.org/10.1080/07391102.2013.817954>.